Nat. Hazards Earth Syst. Sci. Discuss., 3, 2709–2737, 2015
www.nat-hazards-earth-syst-sci-discuss.net/3/2709/2015/
doi:10.5194/nhessd-3-2709-2015

Natural Hazards and Earth System Sciences
Open Access
Discussions

Infrasound array criteria for automatic detection and front velocity estimation of snow avalanches: towards a real-time early-warning system

E. Marchetti[1], **M. Ripepe**[1], **G. Ulivieri**[2], **and A. Kogelnig**[3]

[1]Depart. of Earth Sciences, University of Firenze, via G. La Pira, 4, 50121, Firenze, Italy
[2]Item s.r.l., via B. Gozzoli, 32, 50124, Firenze, Italy
[3]Wyssen Avalanche Control AG, Feld 1, 3713 Reichenbach, Switzerland

Received: 11 March 2015 – Accepted: 26 March 2015 – Published: 17 April 2015

Correspondence to: E. Marchetti (emanuele.marchetti@unifi.it)

Published by Copernicus Publications on behalf of the European Geosciences Union.

Abstract

Avalanche risk management is strongly related to the ability to identify and timely report the occurrence of snow avalanches. Infrasound has been applied to avalanche research and monitoring for the last 20 years but it never turned into an operational tool for the ambiguity to identify clear signals related to avalanches. We present here a new method based on the analysis of infrasound signals recorded by a small aperture array in Ischgl (Austria), which overcome now this limit. The method is based on array derived wave parameters, such as back-azimuth and apparent velocity. The method defines threshold criteria for automatic avalanche identification considering avalanches as a moving source of infrasound. We validate efficiency of the automatic infrasound detection with continuous observations with Doppler Radar and we show how dynamics parameters such as the velocity of a snow avalanche in any given path around the array can be efficiently derived. Our results indicate that a proper infrasound array analysis allows a robust, real-time, remote detection of snow avalanches that could thus contribute significantly to avalanche forecast and risk management.

1 Introduction

Operational avalanche forecast is based on the combination of observations and models of the snowpack and weather, which are validated by on-site observation of avalanche occurrence (McClung and Schaerer, 2006). Natural avalanche activity is a clear sign of instability and is thus often considered as the best warning for further events. However, avalanche activity estimated by visual observations is limited by bad weather and is impossible at night. This prevents usually to know the exact time of occurrence of the event, thus resulting in a poor correlation with the forecast models and a poor estimate of the danger (Schweizer et al., 2003). For this reason, the precise timing of avalanche activity available also at night or during periods of poor visibility and in remote areas would significantly improve operational avalanche forecasting.

NHESSD

3, 2709–2737, 2015

Videogrammetry (e.g. Vallet et al., 2004) and radars (e.g. Gubler and Hiller, 1984) are among the most common geophysical methods to detect snow avalanches. They measure directly the physical characteristics of an avalanche front but are limited to single paths analysis. Radar measurements of a snow avalanches are considered extremely reliable, being able to measure directly the front velocity of the flow in different range gates and providing an estimate of the avalanche size and the precise time of occurrence of an event. Doppler radars are commonly used to notify avalanche occurrence in real time and are used both for risk management and operational avalanche forecasting (Kogelnig et al., 2012). This technique is however limited to one single avalanche path thus resulting in quite high operational costs.

Infrasound (e.g. Bedard, 1989) and seismic observations (e.g. Schaerer and Salway, 1980) are measuring the energy radiated by the avalanche respectively in the atmosphere and in the ground, and are able to detect snow avalanches over large areas and moving along multiple paths. These different monitoring techniques have been used both during temporary experiments or operationally for real-time nowcasting.

Seismic measurements are widely used both for monitoring and research on snow avalanches in many countries worldwide (e.g. Schaerer and Salway, 1980; Kishimura and Izumi, 1997; Leprette et al., 1998; Surinach et al., 2000; van Herwijnen and Schweizer, 2011). Seismic observations provide exact time of occurrence of snow avalanches regardless of the visibility conditions. Seismic measurements have also been used extensively to investigate avalanche dynamics and characteristics by using multiple sensors along a single avalanche paths (e.g. Sabot et al., 1998; Vilajosana et al., 2007). More recently, seismic arrays have been shown to allow accurate location of snow avalanches and evaluation of avalanche front speed also at distances of ~ 3 km (Lacroix et al., 2012).

The use of infrasound for avalanche monitoring has been increasing rapidly in the last decades, with significant improvements also on avalanche dynamics research (Bedard, 1989; Chritin et al., 1996; Adam et al., 1998; Comey and Mendenhall, 2004; Scott et al., 2007; Ulivieri et al., 2011; Kogelnig et al., 2011; Havens et al., 2014;

NHESSD
3, 2709–2737, 2015

Thüring et al., 2015). After the initial works with single infrasound sensors (e.g. Bedard, 1989), the use of infrasound arrays has improved significant the signal-to-noise ratio (e.g. Scott et al., 2007; Ulivieri et al., 2011; Havens et al., 2014), thus resulting into a larger efficiency of infrasound in detecting snow avalanches even at larger (few km) distances. Array processing techniques showed that back-azimuth and apparent velocity of infrasound generated by snow avalanches nicely trace the downhill moving front also at a source-to-receiver distance of 2 km (Ulivieri et al., 2011) and can be used to evaluate avalanche front velocity (Havens et al., 2014). Recently, a network of 3 infrasound arrays deployed in three different valleys in Valle d'Aosta, Italy, allowed Ulivieri et al. (2012) to detect and locate size 3 avalanche at a source-to-receiver distance of ~ 20 km.

The use of infrasound array as monitoring tool for automatic identification of signals from snow avalanches is not fully addressed yet. Scott et al. (2007) showed how array analysis allows increasing the signal-to-noise ratio of infrasound radiated by snow avalanches to support automatic avalanche identification. Ulivieri et al. (2011) first compared results from array analysis of infrasound collected during 2009–2010 winter season and avalanche activity in the area, while more recently Thüring et al. (2015) showed results of supervised machine learning analysis applied to infrasound data recorded during 2011–2012 winter season in Eastern Swiss Alp. However, a systematic comparison of automatic avalanche identification with infrasound data and real avalanche activity is still missing. This is mainly because automatic identification of snow avalanches based on infrasonic waveform can be extremely ambiguous and still requires careful analysis. Snow avalanche are typically recorded as emergent, long-lasting (tens of seconds), infrasonic signal peaking typically at 1–5 Hz (Bedard, 1989; Ulivieri et al., 2011), and a similar infrasonic waveform might result from a wide variety of, natural (earthquakes, meteors, thunders) or anthropogenic (traffic, explosions) source processes.

In this work we present results obtained with an infrasound array, which operated during the 2012–2013 winter season near Ischgl (Paznaun valley, Austria), monitoring

NHESSD
3, 2709–2737, 2015

events from the Grosstal avalanche where spontaneous and controlled events typically occur every year (Jöbstl et al., 2014). Grosstal avalanche is monitored permanently with a pulsed Doppler radar (Kogelnig et al., 2012) which is here used to evaluate the efficiency of the infrasound array techniques to automatically detect events as well as to derive kinetic parameters of snow avalanches. We show how infrasound can be efficiently used as a real-time early-warning system over large areas.

2 The Grosstal avalanche

The Grosstal avalanche, positioned on the northern flank of the Paznaun valley near the town of Ischgl (Austria), is typically characterised by the occurrence of several events/year (Jöbstl et al., 2014), with avalanches reaching the Silvretta road every ten years (Fig. 1). The avalanche has a starting zone of 160 000 m^2 and a path length of 1800 m from the release area (2250 m a.s.l.) down to the bottom of the valley (1360 m a.s.l.).

Between December 2012 and March 2013 avalanche activity in the Paznaun valley was moderate and controlled avalanche release was performed regularly, both in the ski resort as well as along the road. The largest event occurred on 23 December 2012, after an intense snowfall, with avalanche deposit almost reaching the Silvretta road (Fig. 1b). In the following sections we present radar observations of the event and compare it with information derived from infrasound array analysis.

2.1 The avalanche radar

The Grosstal avalanche is permanently monitored with pulsed Doppler radar, which can reliably detect avalanche activity up to distances of 2.5 km and is able to measure velocity ranging between 0.3 and 80 m s^{-1} in 9 different range gates (Kogelnig et al., 2012). In the specific case of the Grosstal avalanche, the radar is facing directly the avalanche path from a distance of ∼ 1800 m and it focuses on the starting zone and

NHESSD
3, 2709–2737, 2015

the upper track. The target area of the radar extends for about ∼ 1000 m of ground distance out of the whole ∼ 1900 m horizontal length of the avalanche path (between ∼ 250 to ∼ 1200 m ground distance from the avalanche starting point) and covers an elevation difference of ∼ 600 m, from 2100 to 1500 m a.s.l. (Fig. 2). Because of the morphology of the channel, the radar is not able to monitor the entire avalanche path (Fig. 2a), and events outside the range gates are not detected (Kogelnig et al., 2012).

The velocity profile measured along the line of sight of the radar for the 23 December 2012, avalanche (Fig. 2c) is showing a continuous increase in velocity up to 15 m s^{-1} within the avalanche detaching area (250–500 m distance from release point), to reach the peak velocity of 18.4 m s^{-1} (850–1050 m ground distance from release point) and then decrease below 15 m s^{-1} afterwards. The lack of data between 700 and 800 m distance corresponds to a blind area of the radar field of view, while the drop of velocity at 1150 m distance depends on the avalanche moving outside the radar field of view. Recorded velocity for the 23 December 2012, events are in the range commonly reported for snow avalanches (Havens et al., 2014).

Radar monitoring of snow avalanche is generally extremely reliable. Its penetration efficiency is limited only by the intense snowfalls and false alarms are reported only in case of strong winds.

2.2 The Ischgl infrasound array, instrument setup and data processing

The infrasound monitoring system deployed in Ischgl (Austria) between December 2012 and March 2013 consisted of a 4-elements infrasound array, with a triangular geometry and an aperture (maximum distance between two elements) of approximately 150 m. The array elements were equipped with differential pressure transducers, with a sensitivity of 25 mV Pa^{-1} in the frequency band 0.01 to 500 Hz. Pressure data were recorded at the sampling rate of 100 Hz with a 24 bits Guralp CMG-DM24 digitiser and GPS time synchronization. The array was installed in the forest close to the Doppler radar and facing different avalanche paths (Fig. 1). The array is deployed in an almost flat surface inclined ∼ 15° towards NW.

NHESSD
3, 2709–2737, 2015

The use of an array instead of a single sensor allows increasing the signal-to-noise ratio and better identifying signal from noise. Array signal processing is based on the assumption that a signal is coherent at different sensors, while noise does not show any correlation. One infrasound detection is defined when, in a given time window (5 s in our case), coherent infrasound signal is recorded across the array and multichannel cross-correlation exceeds a fixed threshold (e.g. Ripepe and Marchetti, 2002). An infrasonic transient, e.g. a snow avalanche, consists typically of multiple detections, as a consequence of event duration and processing windowing (Fig. 3).

Following Ulivieri et al. (2011), the time shifts dt_{ij} between different couples of sensors (i, j) is used to derive the infrasonic ray path of a planar wavefield propagating across the array. This is fully described in terms of back-azimuth (az) and apparent velocity (c_a), where back-azimuth identifies the direction from where the signal is coming from and apparent velocity is reflecting the elevation of the infrasonic source

$$c_a = \frac{c}{\sin(\gamma)}, \quad (1)$$

where, γ is the infrasonic take-off angle, defined as the angle between the infrasonic ray and the normal vector to the surface represented by the array plane, while c is the sound propagation velocity at local temperature and humidity. It is clear from Eq. (1) that the apparent velocity for a linear ray path depends on the elevation of the source.

In the case of a source located right above the array the take-off angle would be zero ($\gamma = 0$) and apparent velocity will be infinite ($c_a = \infty$) consistent with a signal being recorded simultaneously by all the elements of the array. In case of a source moving downhill, such as a snow avalanche, source elevation will decrease, take-off angle will increase and a negative gradient of apparent velocity will be expected.

In the specific case of the Grosstal avalanche remotely controlled explosive activity is performed regularly from fixed stations (Kogelnig et al., 2012) deployed in the avalanche starting area at a distance of ~ 1800 m from the infrasound array. The infrasound detection of such explosive events was used to estimate an error of infrasound back-azimuth of $< 1^{\circ}$.

NHESSD
3, 2709–2737, 2015

The infrasonic record of the 23 December 2012 Grosstal avalanche (Fig. 3) shows several detections with back-azimuth and apparent velocity derived by array processing. The many detections are a consequence of the signal windowing (5 s) and show a continuous migration of back-azimuth (from 309 to 330° N) of ∼ 20° and a reduction of apparent velocity from 460 to 330 m s^{-1} as expected for a downhill moving front. These measured value of apparent velocity are consistent with the Grosstal avalanche path. The elevation difference (∼ 850 m) and ground distance (∼ 1800) between the Grosstal avalanche release zone results into a take-off angle of 64°, which reduces to ∼ 49° once the ∼ 15° inclination of the array is considered. This value corresponds to an apparent velocity of 440 m s^{-1}, assuming a sound propagation velocity of 333 m s^{-1} at ambient temperature of 3 °C, which is in quite good agreement with the value of 460 m s^{-1} derived from infrasound array analysis.

Infrasound produced by an avalanche is thus recorded with peculiar values of back-azimuth and apparent velocity that are reflecting the geometry of the avalanche path as well as the evolution of the avalanche front (Fig. 3). Accordingly, we suggest that infrasound array analysis can contribute both to the study of the avalanche dynamics, in terms of the time-varying wave parameters, as well as to remotely identify event occurrence, with direct effects both in research and monitoring. These two aspects are further discussed in the following sections.

3 Avalanche dynamics and evolution inferred from infrasound observations

The infrasound signal of the 23 December 2012, Grosstal avalanche shows three major phases. The first phase lasts approximately ∼ 50 s (from 01:18:35 to 01:19:25 UTC in Fig. 3a) with the peak pressure amplitude of 1.2 Pa, shows a back-azimuth rotation of ∼ 10° (from 309 to 320° N) and a decay of apparent velocity from ∼ 460 m s^{-1} to ∼ 360 m s^{-1} (Fig. 3a). The second phase is lasting ∼ 65 s (from 01:19:25 to 01:20:30 UTC in Fig. 3a) and is characterized by a lower amplitude (∼ 0.5 Pa) and stable values of back-azimuth at 318° N and apparent velocity at 360 m s^{-1}. The third phase is lasting

NHESSD
3, 2709–2737, 2015

~ 100 s (from 01:20:45 to 01:22:30 UTC in Fig. 3a), shows lower amplitude (< 0.1 Pa) stable values of apparent velocity at $\sim 330\,\mathrm{m\,s^{-1}}$ while back-azimuth keeps rotating of 10 more additional degrees from 320 to 330° N (Phase 3 in Fig. 3). This pattern of back-azimuth and apparent velocity is reflecting the avalanche dynamics in terms of extended moving source radiating infrasound during different stages of the flow.

The first phase is likely dominated by infrasound produced by the avalanche front and changes in the back-azimuth and apparent velocity are reflecting the front trajectory. This phase is indeed characterized by back-azimuth rotating from 309 to 320° N and this interval matches most of the avalanche path (Fig. 4). The stable position of the infrasound source during the second phase could be explained as the rapid deceleration of the avalanche flow induced by the change of topographic slope (Delle Donne et al., 2014). The third phase, which strongly recalls infrasonic waveforms recorded for snow avalanches at the Vallée del La Sionne test site and interpreted as being produced by the dynamics of avalanche deposition in the run-out zone (Kogelnig et al., 2011). This third phase is likely to be produced by a source extending horizontally (back-azimuth varies between 320 and 330° N) but not vertically (stable apparent velocity) and is possibly reflecting the accumulation of snow deposits in the valley (Fig. 1a).

In order to fully understand the meaning of these results, it is important to keep in mind that array analysis allows detecting the most energetic source of infrasound recorded at any given time. If signals from multiple sources is recorded at the same time, only the most energetic signal will be detected. Accordingly, it is reasonable to assume that despite snow deposit accumulation in the valley starts immediately when the avalanche front reaches the valley (i.e. at the end of the first phase, for back-azimuth value of 320° N) it is likely that it will not be detected by the array processing until the larger amplitude infrasound radiated during phase 2 of the avalanche is eventually over.

NHESSD
3, 2709–2737, 2015

Comparison of infrasound and radar observation to retrieve avalanche propagation velocity

Infrasound has been successfully used to track extended down-hill moving sources, proving its efficiency to monitor density currents flows (Ripepe et al., 2010; Delle Donne et al., 2014). Ulivieri et al. (2011) tracked the motion of an avalanche front at a source-to-receiver distance of 2 km with infrasonic back-azimuth and compared it to video imagery showing that infrasonic back-azimuth nicely matches the migration of the avalanche front and could be used to derive infrasound velocity. More recently Havens et al. (2014) evaluated instantaneous front velocity of a snow avalanches by applying Fisher-statistics of infrasound array observations along the section of the avalanche path. Here we present a procedure to derive automatically the avalanche front velocity directly from infrasound array observations.

From a digital elevation map (DEM) of the area with 10 m resolution we calculate the avalanche path and evaluate for each point the absolute position (x_i, y_i, z_i) and the expected back-azimuth (az_i) (Fig. 4a). From the position of the avalanche path in space, we evaluate the horizontal (h_i) and slant distance (l_i) between successive points ($i-1$ and i) along the path and the corresponding back-azimuth at the array:

$$\begin{cases} h_i = \sqrt{(x_i - x_{i-1})^2 + (y_i - y_{i-1})^2} \\ l_i = \sqrt{(z_i - z_{i-1})^2 + h_i^2} \\ az_i = \tan^{-1}\left(\frac{x_i - x_{a4}}{y_i - y_{a4}}\right) \end{cases}, \quad (2)$$

where x_{a4} and y_{a4} are the coordinates of the central element of the array. The slant (L) and ground distance (H) are defined by the sum of the different portions along the whole avalanche path:

NHESSD
3, 2709–2737, 2015

$$\begin{cases} H = \sum_{i}^{N} h_i \\ L = \sum_{i}^{N} l_i \end{cases} . \quad (3)$$

This geometrical discretization of the avalanche path allows to link infrasonic back-azimuth (az_i) with the position of the avalanche front along the path (x_i, y_i, z_i) and thus to relate variation of infrasonic back-azimuth ($\Delta az_i = az_i - az_j$) to distances ($h_i$, l_i) travelled by the avalanche front in time (Fig. 4b).

It is clear from Fig. 4 that the mutual positions of the avalanche path and the infrasound array result into a non-homogeneous azimuthal resolution of the path, with the lowest resolution for the avalanche starting area, where a distance of 400–500 m is limited to back-azimuth variation $< 1^\circ$ (309–310° N, Fig. 4b), it is significantly better in the avalanche main channel, where an horizontal distance of ~ 800 m is tracked by a back-azimuth interval of $\sim 10^\circ$ (310–320° N) and it is maximum in the accumulation zone which is tracked by a back-azimuth variation exceeding 10° (320–330° N).

Once the geometrical relation between infrasound back-azimuth and distance along the avalanche path is derived (Eq. 2), we evaluate the avalanche front velocity as a function of time. Variations of infrasonic back-azimuth can easily be converted into the distance travelled by the front as a function of time thus providing the instantaneous front velocity (Fig. 5).

This procedure, once applied to the infrasonic detections of the 23 December 2012, Grosstal avalanches, shows instantaneous velocities ranging from ~ 10 up to $35\,m\,s^{-1}$ (mean $20\,m\,s^{-1}$) at the beginning of the event (01:19:00–01:19:30 UTC). Infrasound derived front velocity becomes stable around $\sim 6\,m\,s^{-1}$ between 01:19:30 and 01:20:30 UTC, when back-azimuth shows a limited rotation from 317 to 319° N. Velocity peaks again at 01:20:30 UTC, reaching values of $22\,m\,s^{-1}$ and then gradually tends to

NHESSD
3, 2709–2737, 2015

zero. This secondary velocity peak, is recorded for back-azimuth rotation from 319 to 322° N, which corresponds to the channel entering into the valley.

Figure 6 shows the comparison between the velocity measured directly by the radar and the velocity derived from infrasound array observations. Despite the generally larger values, possibly to be explained being the velocity along the radar line of sight an underestimate of the real front velocity, infrasound derived velocity appear to match the general trend of radar measurement. For ground distances ranging between 650 and 1100, the difference between velocity derived from infrasound and measured by the radar peaks at 13 $m\,s^{-1}$ but is generally below 3 $m\,s^{-1}$. Moreover, infrasound analysis extends radar measurements outside the radar field of view along the avalanche path (between 700 and 800 m of ground distance) and in the avalanche depositional area (> 1100 m ground distance). The good matching of the results suggests that the velocity of an avalanche front can be derived from infrasound observation, once the topographic profile of the avalanche path is known. Our analysis provides the evidence that infrasound analysis can be efficiently used to estimate the front velocity of fast moving density currents (Yamasato, 1997; Ripepe et al., 2009; Delle Donne et al., 2014; Havens et al., 2014) and improves the procedure also for avalanche paths that are not optimally located with respect to the array.

4 Automatic avalanche identification

Infrasound array analysis is able of tracking a snow avalanche and to derive the avalanche front velocity (Figs. 5 and 6) with strong implications on the study of avalanche dynamics.

Based on previous analysis of the Grosstal avalanche, we show how some of the peculiar features described above can be used as criteria for a robust automatic identification of snow avalanche events. Infrasound array analysis was applied to data collected at Ischgl during December 2012–March and band-pass filtered between 0.5 and 20 Hz, leading to a total of 31 770 infrasonic detections, corresponding to a mean rate

NHESSD
3, 2709–2737, 2015

of 262 detections day^{-1} (Fig. 7). Amplitude of infrasonic detections is generally small and limited to 0.2 Pa, with higher values at the array being commonly recorded for controlled explosions. While back-azimuth of infrasound detections tend to cluster in the 200–330° N range, the mean propagation velocity of 330 m s^{-1} is consistent with an air temperature of ∼ 0 °C, in agreement with what expected during the winter at this latitude.

Many of the observed detections might result from a wide range of sources producing infrasound in the 0.5–20 Hz frequency range typically radiated by snow avalanches (e.g. Bedard, 1989) and acting at various ranges all around the array. These might include microbarom, severe weather (i.e. thunderstorms and lightnings), anthropogenic sources (industrial plants, airplanes) and other natural processes (e.g. meteorites, earthquakes).

Based on the evidence that snow avalanches are detected with predictable behaviour of back-azimuth and apparent velocity (Figs. 4 and 5) we extracted from the whole dataset (Fig. 7) all possible avalanches that occurred from Grosstal. The threshold criteria used to automatically detect avalanches from Grosstal are the following: (i) detections must show a back-azimuth rotation > 5° and have values included in the 310–320° N range; (ii) decrease of apparent velocity of > 10 m s^{-1}; (iii) duration of the event must be longer than 10 s; (iv) peak amplitude at the array must be larger than 0.05 Pa. While the last two criteria are related to the size of the event and limit the analysis to the most significant events, the first two criteria are reflecting the kinematics nature of avalanches of being a moving source of infrasound and limit the analysis to Grosstal avalanche path.

Out of the 31 700 infrasound detections recorded between December 2012 and March 2013, only three events appear to match these threshold criteria (Fig. 8). All appear to show the same kinematic behaviour. The 10 December 2012, infrasound event shows a smaller back-azimuth variation, of ∼ 5° limited to 320° N, and its duration (∼ 80 s) and is significantly shorter than the others (> 200 s), indicating a shorter run-out of the event.

NHESSD
3, 2709–2737, 2015

While two of the events extracted automatically (23 December 2012 and 11 March 2013) are consistent with avalanches also recorded by the radar, only for the first event (10 December 2012) we have no visual observations, nor radar detections. However, at the time of the event snowfall was intense and this might have prevented the observation of the deposit and limited the radar efficiency, thus it is not straightforward to exclude the occurrence of an event. Based on this result, we can conclude that the automatic avalanche identification based on array processing analysis did not produce any false alarm, with respect to the radar, for avalanches occurring from Grosstal.

The good results obtained for the Grosstal avalanche (Fig. 8), allowed us to extend the automatic thresholds in order to detect snow avalanches occurring also all around the array. In particular threshold criteria have been expanded as follow: (i) detections must show a back-azimuth rotation $> 5^{\circ}$; (ii) decrease of apparent velocity of $> 10\,\mathrm{m\,s^{-1}}$; (iii) duration of the event can be longer than 10 s; (iv) peak amplitude at the array must be larger than 0.05 Pa.

New thresholds expand the number of events to only 103 out of the 31 770 detections. All the events have a back-azimuth rotation between 5 and 60° (mean = 10°) and a mean decrease of apparent velocity of $\sim 40\,\mathrm{m\,s^{-1}}$. Most of the automatically extracted events are located west of the array within a main back-azimuth interval from 170 to 360° N (Fig. 9), consistent with avalanches released from the northern (240–20° N) and southern flank (170–240° N) of the valley. Very few infrasonic signals have back-azimuth ranging between 60 and 170° N, which is in agreement with a topographic sector where no avalanche have been observed.

According to this infrasonic analysis avalanche activity peaked on 23 December 2012, with a maximum of $15\,\mathrm{events\,day^{-1}}$ and exceed $5\,\mathrm{events\,day^{-1}}$ on 10, 11, 28 December 2012 and 12 March 2013 (Fig. 9c), when also avalanches from Grosstal did actually occur (Fig. 8).

For this specific case of the 22–23 December 2012, peak activity, 16 infrasonic events (Fig. 10) were automatically identified during a 6 h-long time period (between

NHESSD
3, 2709–2737, 2015

21:00 UTC of 22 December and 03:00 UTC of 23 December). These events showed back-azimuth consistent with avalanches occurring both in the northern (around Grosstal avalanche) and southern flank (around Hoherzug avalanche) of the Paznaun valley. In the morning, deposits from at least six avalanches from the avalanche paths around Grosstal could be observed, indicating the high efficiency of our automatic system to locate and identify infrasound generated by snow avalanches.

5 Discussion and conclusions

During the last 10 years, infrasound analysis of snow avalanches is becoming one of the most promising tool to monitor snow avalanches (e.g. Scott et al., 2007; Ulivieri et al., 2011; Havens et al., 2014; Thüring et al., 2015), but the use of infrasonic arrays as permanent monitoring tool is still limited to temporary experimental sites. Unlike radars, which target a specific single avalanche path, infrasound array analysis can be applied to multiple paths covering large areas around the array, with a resolution depending on the mutual position of the array and the avalanche path (Fig. 4). However, while radar monitoring is considered as a reliable monitoring system for snow avalanches, the utility of infrasound is still debated because the difficulties of recognising univocally signals generated by snow avalanches are believed to produce many false alarms. Despite a systematic field validation should be still required, the results presented so far already highlight the potential benefit of infrasound array analysis for the research of avalanche dynamics as well as avalanche remote detection and risk management.

A snow avalanche front moving downhill behaves as a moving linear source of infrasound, which is continuously changing its position in the 3-D space. We show here that infrasound is able to follow these changes in terms of rotation of the propagation back-azimuth and of decreasing in the apparent velocity. These two parameters are reflecting an extended downhill moving source and are thus distinctive of snow avalanches as well as most of the density currents able to generate infrasound (Ripepe et al., 2009;

NHESSD
3, 2709–2737, 2015

Delle Donne et al., 2014; Havens et al., 2014) and can be used to efficiently monitor avalanches automatically and in real-time.

The migration of infrasonic back-azimuth projected on the topography provides an estimate of the instantaneous velocity of the moving front (Figs. 4 and 5). We showed how infrasound recorded with a small aperture array can be used to estimate the avalanche front velocity, which nicely fits with velocity measured directly by a pulsed Doppler radar. We suggest that this procedure can be applied to multiple paths around the array and it provides reliable results even if the path geometry is not optimal in terms of back-azimuth to the array, as in the case of the Grosstal avalanche.

Avalanche kinematics can be used to fix threshold criteria for automatic identification of infrasonic signals generated by avalanches from various paths around the array, once back-azimuth and apparent velocity of infrasonic detections are properly analysed (Fig. 8). Infrasound can reliably provide the number and the time of occurrence of snow avalanches occurring all around the array (Fig. 9), which represent key information for a proper validation of avalanche forecast models (Schweizer and van Herwjinen, 2013).

Snow avalanches can be represented in terms of moving sources, characterised by specific values of back-azimuth and apparent velocity, which make the procedure of automatic event detection extremely reliable, suggesting how infrasound could be used also for real-time avalanche risk management. The avalanche activity near Ischgl during the night of 22–23 December 2012, was detected by the radar only at 01:18 UTC of 23 December, while infrasound array analysis provide an evidence that avalanche activity increased in the area already ~ 3–4 h before (Fig. 10). In this specific case, an infrasound array monitoring system might have delivered automatically and in real-time an early warning of increased avalanche activity, with strong impact on risk management.

Acknowledgements. We thank the Ischgl Avalanche Team and in particular Albert Siegele for providing field and observational data of avalanches released from Grosstal. E. Marchetti and M. Ripepe were supported by the European Union ARISE FP7 project (GA 284387).

NHESSD
3, 2709–2737, 2015

References

Adam, V., Chritin, V., Rossi, M., and Van Lancker, E.: Infrasonic monitoring of snow-avalanche activity: what do we know and where do we go from here?, Ann. Glaciol., 26, 324–328, 1998.

Bedard, A.: Detection of avalanches using atmospheric infrasound, in: Proceedings of the Western Snow Conference, edited by: Shafer, B., Western Snow Conference, Colorado State University, 52–58, 1989.

Chritin, V., Rossi, M., and Bolognesi, R.: Acoustic detection system for operational avalanche forecasting, in: Proceeding of International Snow Science Workshop, 6–11 October 1996, Banff, Alberta, 129–133, 1996.

Comey, R. H. and Mendenhall, T.: Recent studies using infrasound sensors to remotely monitor avalanche activity, in: Proceeding of International Snow Science Workshop, 19–24 September 2004, Jackson, WY, 640–646, 2004.

Delle Donne, D., Ripepe, M., De Angelis, S., Cole, P. D., Lacanna, G., Poggi, P., and Stewart, R.: Thermal, acoustic and seismic signals from pyroclastic density currents and vulcanian explosions at Soufrie're Hills Volcano, Montserrat, in: The Eruption of Soufrie're Hills Volcano, Montserrat from 2000 to 2010, edited by: Wadge, G., Robertson, R. E. A., and Voight, B., Geological Society, London, Memoirs, 39, 167–176, doi:10.1144/M39.9, 2014.

Gubler, H. and Hiller, H.: The use of microwave FMCW radar in snow and avalanche research, Cold. Reg. Sci. Technol., 9, 109–119, 1984.

Jöbstl, L., Studeregger, A., Wurzer, A., Stock, D., and Koschuh, R.: Analysis of detected avalanches using meteorological data of nearby monitoring stations in Ischgl, Austria, J. Environ. Sci. Eng. B, 3, 87–90, 2014.

Havens, S., Marshall, H. P., Johnson, J. B., and Nicholson, B.: Calculating the velocity of a fast-moving snow avalanche using an infrasound array, Geophys. Res. Lett., 41, 6191–6198, doi:10.1002/2014GL061254, 2014.

Kishimura, K. and Izumi, K.: Seismic signals induced by snow avalanche flows, Nat. Hazards, 15, 89–100, 1997.

Kogelnig, A., Suriñach, E., Vilajosana, I., Hübl, J., Sovilla, B., Hiller, M., and Dufour, F.: On the complementariness of infrasound and seismic sensors for monitoring snow avalanches, Nat. Hazards Earth Syst. Sci., 11, 2355–2370, doi:10.5194/nhess-11-2355-2011, 2011.

NHESSD
3, 2709–2737, 2015

Kogelnig, A., Wyssen, S., and Pichler, J.: Artificial release and detection of avalanches: managing avalanche risk on traffic infrastructures: a case study from Austria, in: Proceedings, 2012 International Snow Science Workshop, Anchorage, Alaska, 535–540, 2012.

Lacroix, P., Grasso, J.-R., Roulle, J., Giraud, G., Goetz, D., Morin, S., and Helmstetter, A.: Monitoring of snow avalanches using a seismic array: location, speed estimation, and relationships to meteorological variables, J. Geophys. Res., 117, F01034, doi:10.1029/2011JF002106, 2012.

Leprette, B., Navarre, J.-P., Panel, J.-M., Touvier, F., Taillefer, A., and Roulle, J.: Prototype for operational seismic detection of natural avalanches, Ann. Glaciol., 26, 313–318, 1998.

McClung, D. and Schaerer, P. A.: The Avalanche Handbook, The Mountaineers Books, Seattle, WA, USA, 2006.

Ripepe, M. and Marchetti, E.: Array tracking of infrasonic sources at Stromboli volcano, Geophys. Res. Lett., 29, 2076, doi:10.1029/2002GL015452, 2002.

Ripepe, M., De Angelis, S., Lacanna, G., Poggi, P., Williams, C., Marchetti, E., Delle Donne, D., and Ulivieri, G.: Tracking pyroclastic flows at Soufriere Hills Volcano, EOS T. Am. Geophys. Un., 90, 229–230, doi:10.1029/2009EO270001, 2009.

Sabot, F., Naaim, M., Granada, F., Surinach, E., Planet-Ladret, P., and Furdada, G.: Study of the avalanche dynamics by means of seismic methods, image processing techniques and numerical models, Ann. Glaciol., 26, 319–323, 1998.

Schaerer, P. and Salway, A.: Seismic and impact-pressure monitoring of flowing avalanches, J. Glaciol., 26, 179–187, 1980.

Schweizer, J. and van Herwijnen, A.: Can near real-time avalanche occurrence data improve avalanche forecasting?, in: Proceedings, 2013 International Snow Science Workshop, Grenoble–Chamonix Mont Blanc, 195–198, 2013.

Schweizer, J., Jamieson, J. B., and Schneebeli, M.: Snow avalanche formation, Rev. Geophys., 41, 1016, doi:10.1029/2002RG000123, 2003.

Scott, E., Hayward, C., Kubichek, R., Hamann, J., and Pierre, J.: Results of recent infrasound avalanche monitoring studies, in: Proceedings, 2004 International Snow Science Workshop, Jackson Hole, Wyoming, 696–704, 2004.

Scott, E. D., Hayward, C. T., Kubichek, R. F., Hamann, J. C., Pierre, J. W., Corney, B., and Mendenhall, T.: Single and multiple sensor identification of avalanche-generated infrasound, Cold Reg. Sci. Technol., 47, 159–170, 2007.

NHESSD

3, 2709–2737, 2015

Surinach, E., Sabot, F., Furtada, G., and Vilaplana, J.: Study of seismic signals on artificially released snow avalanches for monitoring purposes, Phys. Chem. Earth Pt. B, 25, 721–727, 2000.

Thüring, M. S., van Herwijnen, A., and Schweizer, J.: Robust snow avalanche detection using supervised machine learning with infrasonic sensor arrays, Cold Reg. Sci. Technol., 111, 60–66, doi:10.1016/j.coldregions.2014.12.014, 2015.

Ulivieri, G., Marchetti, E., Ripepe, M., Chiambretti, I., De Rosa, G., and Segor, V.: Monitoring snow avalanches in northwestern Italian Alps using an infrasound array, Cold Reg. Sci. Technol., 69, 177–183, doi:10.1016/j.coldregions.2011.09.006, 2011.

Ulivieri, G., Marchetti, E., Ripepe, M., Chiambretti, I., and Segor, V.: Infrasonic monitoring of snow avalanches in the Alps, in: Proceedings, 2012 International Snow Science Workshop, Anchorage, Alaska, 723–728, 2012.

Vallet, J., Turnbull, B., Joly, S., and Dufour, F.: Observations on powder snow avalanches using videogrammetry, Cold Reg. Sci. Technol., 39, 153–159, doi:10.1016/j.coldregions.2004.05.004, 2004.

Van Herwijnen, A. and Schweizer, J.: Monitoring avalanche activity using a seismic sensor, Cold. Reg. Sci. Technol., 69, 165–176, doi:10.1016/j.coldregions.2011.06.008, 2011.

Vilajosana, I., Khazaradze, G., Surinach, E., Lied, E., and Kristensen, K.: Snow avalanche speed determination using seismic methods, Cold Reg. Sci. Technol., 49, 2–10, doi:10.1016/j.coldregions.2006.09.007, 2007.

Yamasato, H.: Quantitative analysis of pyroclastic flows using infrasonic and seismic data at Unzen Volcano, Japan, J. Phys. Earth, 45, 1997, 397–416, 1997.

NHESSD

3, 2709–2737, 2015

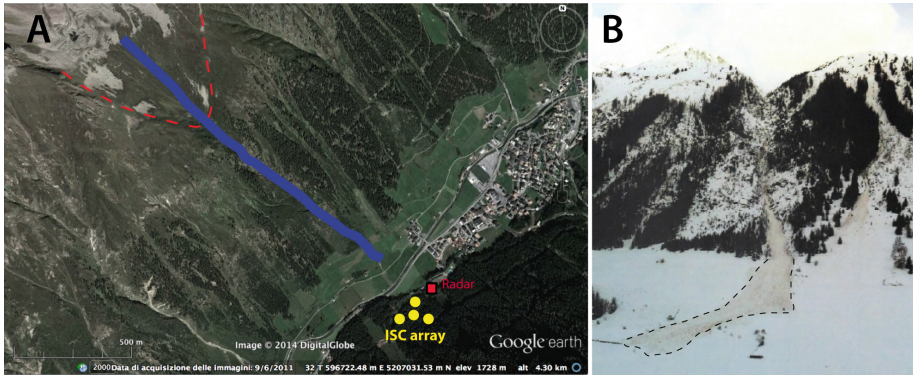

Figure 1. (a) Google Earth view of the Paznaun valley near Ischgl (Austria), showing the position of the Grosstal avalanche path (blue line) and starting area (dashed red line), position of the monitoring radar (red square) and of the infrasound array (yellow circles) deployed during the 2012/2013 winter season. **(b)** Picture of the 23 December 2012, Grosstal avalanche taken in the morning ~ 7–8 h after the event.

NHESSD
3, 2709–2737, 2015

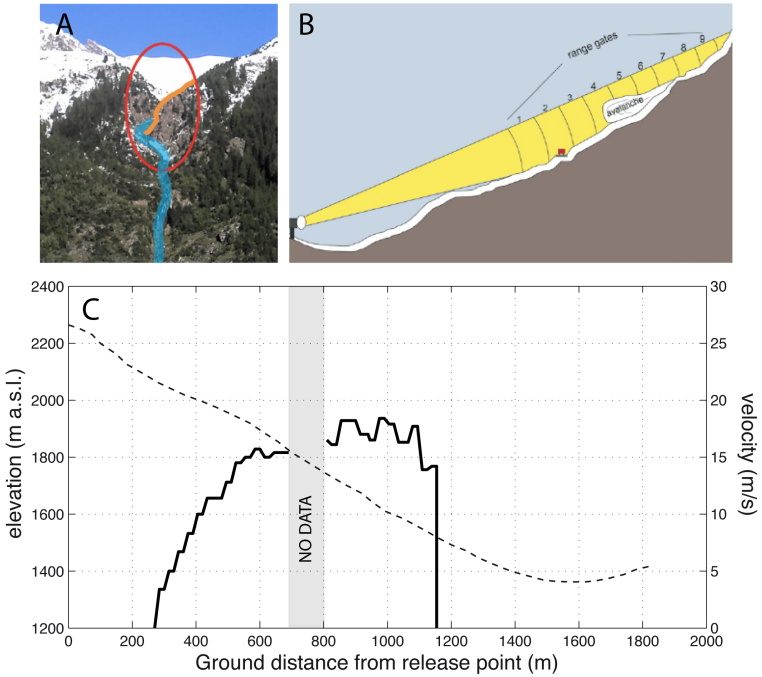

Figure 2. View of the Grosstal avalanche path (blue line) from the monitoring radar **(a)**. The red circle identifies the sector of the avalanche path monitored by the radar, while the orange line identifies a ridge that prevents monitoring of the path between 700 and 800 m ground distance from release point. The radar is able to detect the moving front of the avalanche in several range gates **(b)** within a ground distance from the release point spanning from ~250 to 1150 m; (red circle in **a**). **(c)** Velocity profile of the 23 December 2012, event as measured by the radar. The avalanche path profile is shown in background (black dashed line). The shadow area results into the decay of velocity between 700 and 800 m ground distance from release point.

NHESSD
3, 2709–2737, 2015

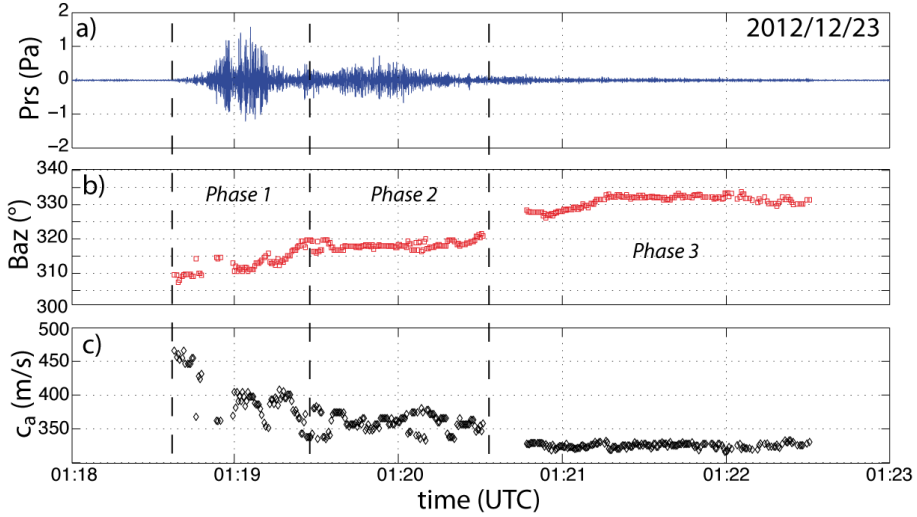

Figure 3. Infrasonic record **(a)**, back-azimuth **(b)** and apparent velocity **(c)** of infrasound detections of 23 December 2012, snow avalanches from Grosstal (Fig. 1). The vertical dashed lines define the three different phases of the signals which are discussed in detail in the text.

NHESSD
3, 2709–2737, 2015

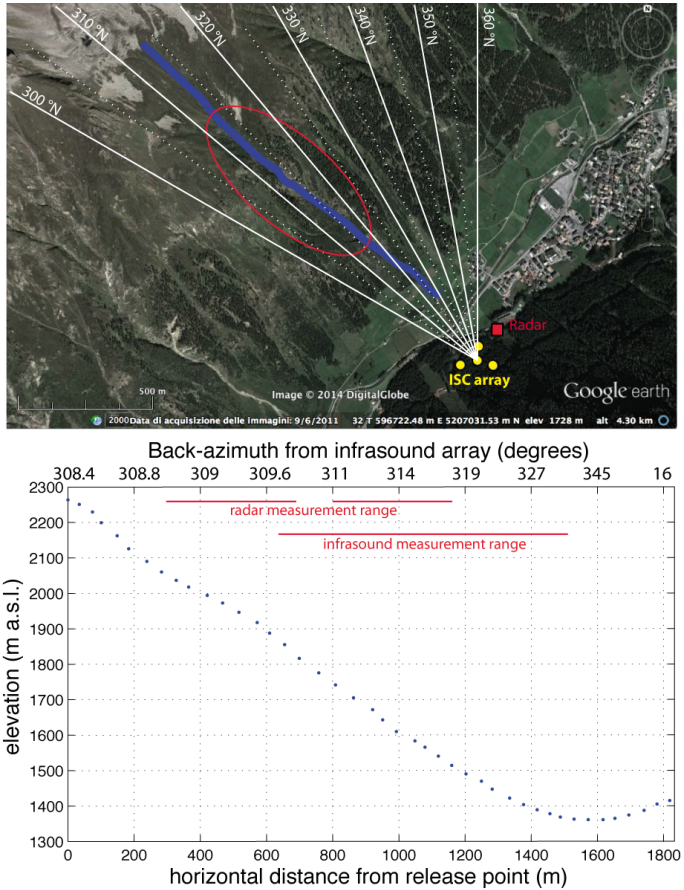

Figure 4. View of the Grosstal avalanche path (blue) showing the theoretical values of back-azimuth to the array (white) and target area of the Doppler radar (red). **(b)** The Grosstal avalanche path as a function of infrasonic back-azimuth to the array and horizontal distance from release point.

NHESSD
3, 2709–2737, 2015

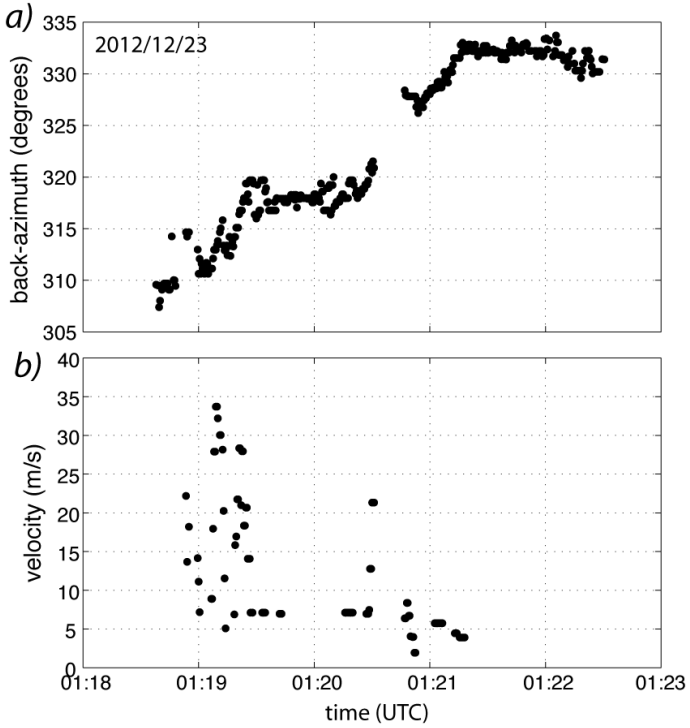

Figure 5. Back azimuth of the 23 December 2012, Grosstal avalanche **(a)** and instantaneous avalanche front velocity **(b)** derived from the infrasound array analysis.

NHESSD
3, 2709–2737, 2015

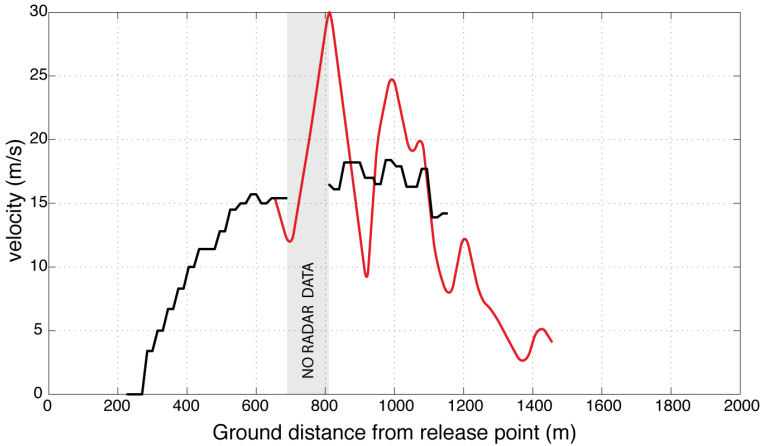

Figure 6. Comparison of avalanche front velocity as measured by the radar (black line) and derived from infrasound array analysis (red line). Grey bars show the velocity of different sectors of the avalanche path derived from infrasound array.

NHESSD
3, 2709–2737, 2015

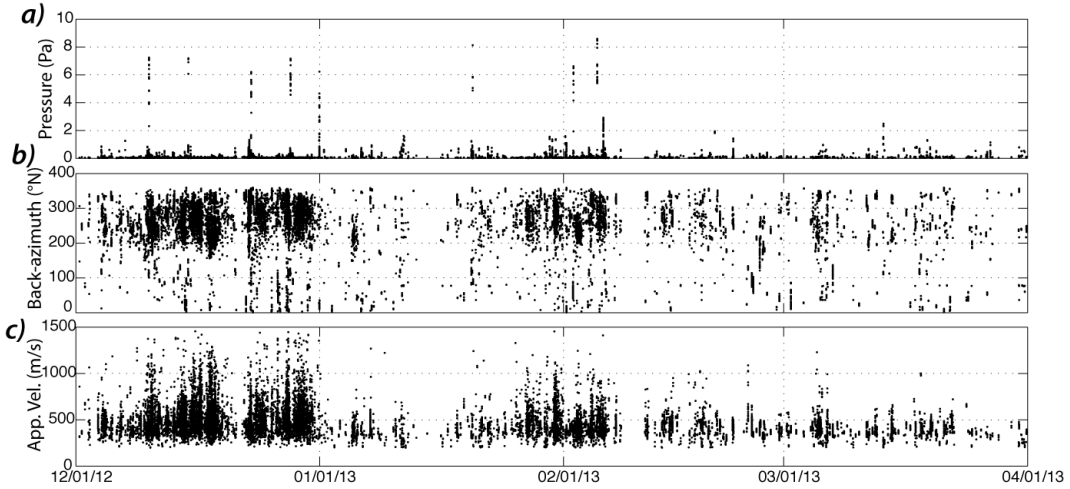

Figure 7. Results of infrasound array processing for the period of analysis (December 2012–March 2013) showing amplitude **(a)**, back-azimuth **(b)** and apparent velocity **(c)** of calculated infrasound detections.

NHESSD
3, 2709–2737, 2015

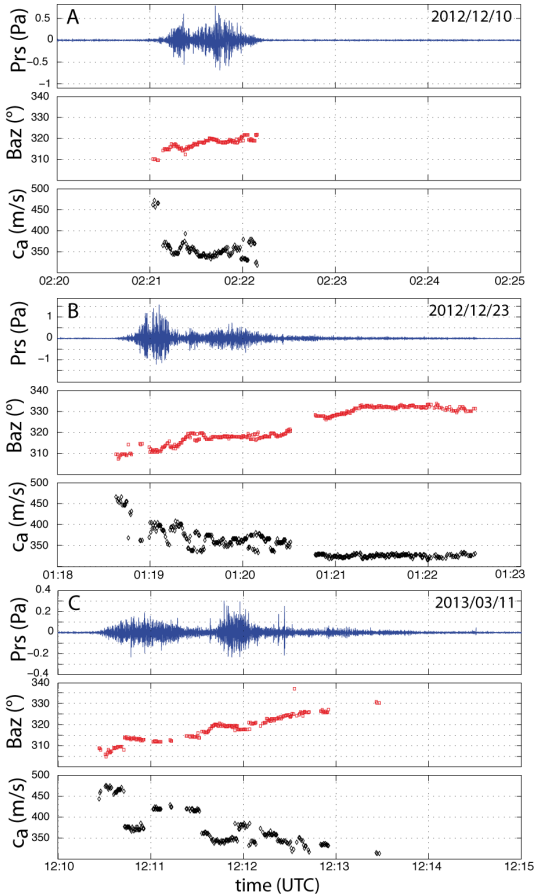

Figure 8. Infrasonic signature at the array (blue), back-azimuth (red) and apparent velocity (black) of infrasound detections for the 3 events extracted automatically from the whole dataset.

NHESSD
3, 2709–2737, 2015

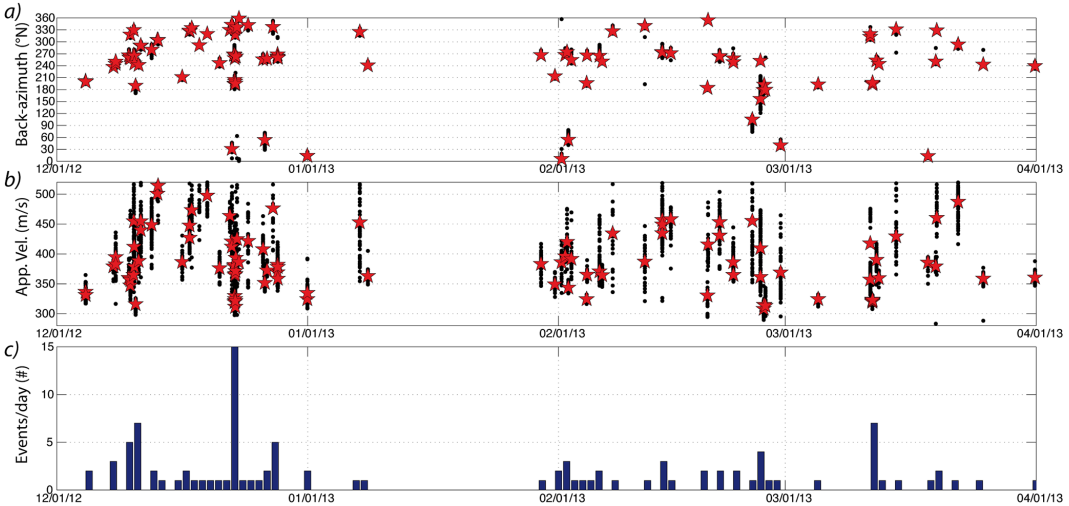

Figure 9. (a) Back-azimuth and apparent velocity **(b)** of infrasonic detections (black dots) of 103 signals (red stars) showing infrasound wave parameters consistent with what expected by snow avalanches identified by the infrasound array between December 2012 and March 2013. **(c)** Number of events day^{-1} during the 2012–2013 winter season.

NHESSD
3, 2709–2737, 2015

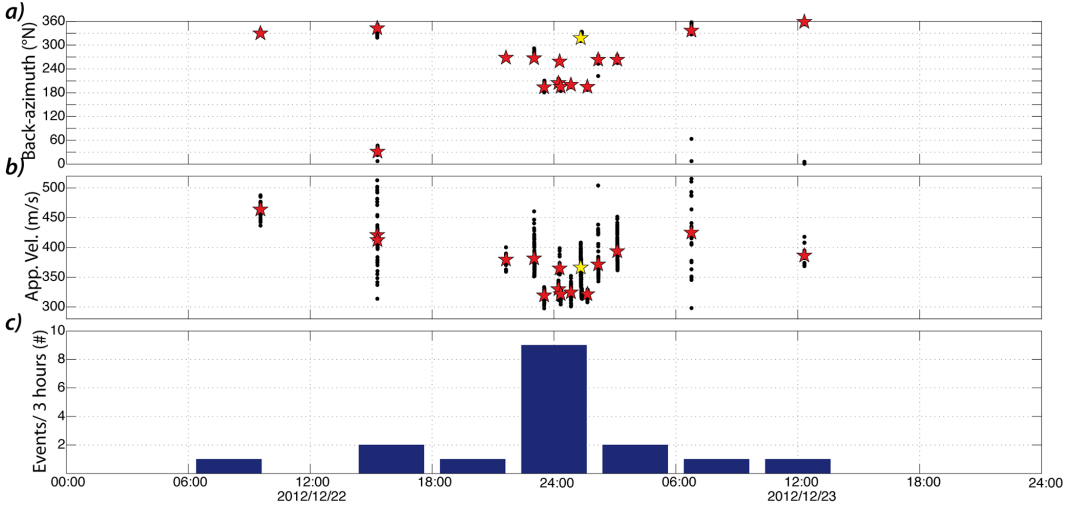

Figure 10. (a) Back-azimuth and apparent velocity **(b)** of infrasonic detections (black dots) for 16 events (stars) recorded during 22 and 23 December 2012. The yellow star corresponds to the 23 December 2012 Grosstal avalanche (Figs. 1–3), which was detected by the radar. Number of events every 3 h **(c)** shows a significant increase since the afternoon of 22 December.

NHESSD
3, 2709–2737, 2015